Perturbed ion current effects on kinetic ballooning mode for different magnetic shears

Y. Li, Y. Xiao*

Institute for Fusion Theory and Simulation, Zhejiang University, Hangzhou,310027, PRC

* (Corresponding author) E-mail: yxiao@zju.edu.cn

Various gyrokinetic simulations suggest that the kinetic ballooning mode instability is sensitive to the numerical implementation of equilibrium magnetic configuration in tokamaks. In this work, the gyrokinetic code GTC is employed to investigate the KBM's sensitivity to equilibrium plasma profiles. An outward radial shift of the radial mode is found for the normal magnetic shear case, but there is no shift if the shear is negative. The simulation results are explained by a linear eigenmode theory. It is found that the observed phenomenon is an effect of the perturbed parallel ion current.

I. INTRODUCTION

The ideal MHD ballooning mode (IBM) in tokamak plasmas is one of the most thoroughly investigated MHD instabilities. It imposes an upper limit for the maximum pressure gradient in the first IBM stability regime, and suggests the existence of a second stability regime arising from the Shafranov shift of the magnetic axis when the plasma pressure gradient is sufficiently high. A closely related mode the kinetic ballooning mode (KBM), which include important kinetic modifications to the IBM code, e.g., the diamagnetic flow, finite Larmor radius effect and wave particle resonance. [1] The KBM physics has been investigated for many years [2, 3] and its physics is still not fully clear. Earlier efforts have been focused on the low-beta, large-aspect-ratio s-α equilibrium model, under the assumptions $\omega \gg k_{\parallel} v_{Ti}$ and

$\omega \ll \omega_{*e}$, where ω is the characteristic frequency of KBM, $k_{\|}$ represents the parallel wavelength, v_{Ti} is the ion thermal speed, and ω_{*e} is the electron diamagnetic frequency .[4] Subsequent works have include the effects of trapped electrons, passing ions, parallel magnetic perturbation etc.. The stability of the KBM has been investigated in the parameter regimes relevant to internal transport barriers (ITB) with negative magnetic shear [5, 6].

Even after one decade of gyrokinetic simulation of KBM [7, 8, 9, 10], detailed understanding and verification between different codes remain challenging. Recently, the properties of the linear the KBM as predicted by different gyrokinetic codes such as GS2, GTC, GYRO, BOUT++ and GENE have been compared [11, 12, 13]. It is realized that the linear KBM, in contrast to the electrostatic modes such as ion temperature gradient (ITG) mode and trapped electron mode (TEM), is extremely sensitive to the equilibrium magnetic configurations implemented in the different codes [13].

In this work, we carry out the KBM simulations using GTC code. It is found that both linear growth rate and real frequency depend on the width of the gradient profile, i.e., effectively the simulation window implemented in the code. In particular, the radial mode structure suffers an outward shift in the normal magnetic shear (i.e., the shear monotonically increases with r, or the poloidal flux ψ_p) case, but there is no shift in the reversed-shear case. We also propose an eigenmode theory that explains this shear-dependent radial mode shift. The perturbed parallel ion current is found to be responsible for the radial mode shift observed in the simulation.

In Section II, we carry out KBM simulations using the GTC code and find the locality of the plasma profile has a strong effect on the linear KBM properties. In Section III, we develop an eigenmode theory and numerically solve the eigenvalue problem to study the linear KBM physics. . In Section IV, we show that the perturbed parallel ion current has a stabilizing effect on the KBM for normal shear, which is responsible for the radially outward shift of the KBM mode structure. In Section V we show that, depending on the magnetic shear, the perturbed parallel ion current can

have quite different effects on the KBM. In Section VI, the relation between the magnetic shear effect and the perturbed parallel ion current effect is verified by the GTC simulation. Section VII gives conclusion and discussion.

II. Plasma Profile Effect on the KBM

As mentioned, the KBM is extremely sensitive to the numerical implementation of the equilibrium magnetic configuration [14]. Here we use the GTC code[14, 15, 16, 17, 18] to study the KBM sensitivity to the numerical implementation of the plasma profile. The GTC code is a global particle-in-cell (PIC) gyrokinetic code which can directly import experimental magnetic equilibrium and profiles as the simulation setup. In order to investigate the numerical plasma profile effect on the KBM instability, an analytical flat gradient profile has been used in the simulation as a reference local model for the plasma profile, as shown in Fig 2(b)-(d) by the dashed lines. The q profile used in the GTC simulations is $q(\psi_p) = q_1 + q_2\left(\frac{\psi_p}{\psi_w}\right) + q_3\left(\frac{\psi_p}{\psi_w}\right)^2$, where q is the safety factor, ψ_p is the poloidal flux, ψ_w is the poloidal flux on the wall, $q_1 = 0.81$, $q_2 = 1.1$, and $q_3 = 1.0$. A local (flat gradient) plasma profile is generally used by the global simulations for verifying the corresponding local theory or the simulation results from the local codes. In the GTC simulation, the temperature and density gradient profiles are assumed to be flat in the central region of the radial domain, namely $L_n^{-1}, L_T{}^{-1} \propto \exp\left[-\left(\frac{r-0.5a}{r_w}\right)^6\right]$, where a is the minor radius, r_w represents the width of the flat region for the gradients, and $L_n^{-1} = -\mathrm{dlnn/dr}$, $L_T^{-1} = -\mathrm{dlnT/dr}$ are the scale lengths of density and temperature, respectively..

Fig. 1 shows the simulation results for three typical toroidal mode numbers and the simulation parameters evaluated at $r = a/2$ are: $\beta = 2.0\%$, $\epsilon = 0.35$, $k_\theta \rho_s = 0.2$ and $q = 1.4$, $s = 0.81$, $\frac{R}{L_n} = 2.2$, $\frac{R}{L_T} = 7.0$, where $s = dlnq/dlnr$ is the magnetic shear, β is the ratio of the plasma pressure to the magnetic pressure.. One can clearly see that the KBM linear frequency and growth rate are sensitive to the

width r_w of the local profile. In Fig. 1, the point r_w =0 corresponds to a global analytic profile for the temperature and density, as shown by the dashed line in Fig. 2(a), where only the peak gradient at $r = a/2$ is the same as the other three local profiles. Both linear frequency and growth rate depend on the width of the local profile and the dependence is more pronounced for larger toroidal mode numbers.

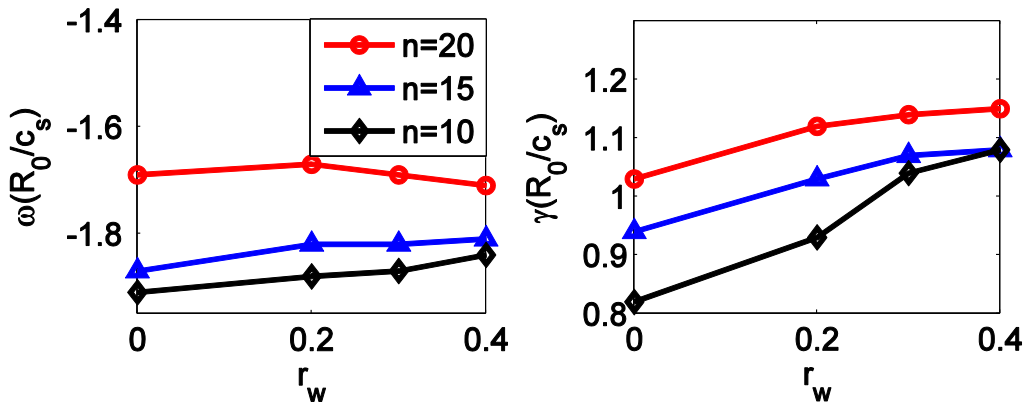

Figure 1: The growth rate and frequency from GTC simulation for $n = 10,15,20$ and $r_w = 0.2a, 0.3a, 0.4a$.

Fig. 2 shows the GTC simulation results for the radial mode structure for different widths of the temperature and density gradient profiles. The toroidal mode number is n=10 and the peak positions corresponds to that of the mode rational surfaces for different poloidal mode numbers. We see that the radial mode structure moves outward as the gradient width r_w increases. It is therefore of interest to find out the cause of this outward shift.

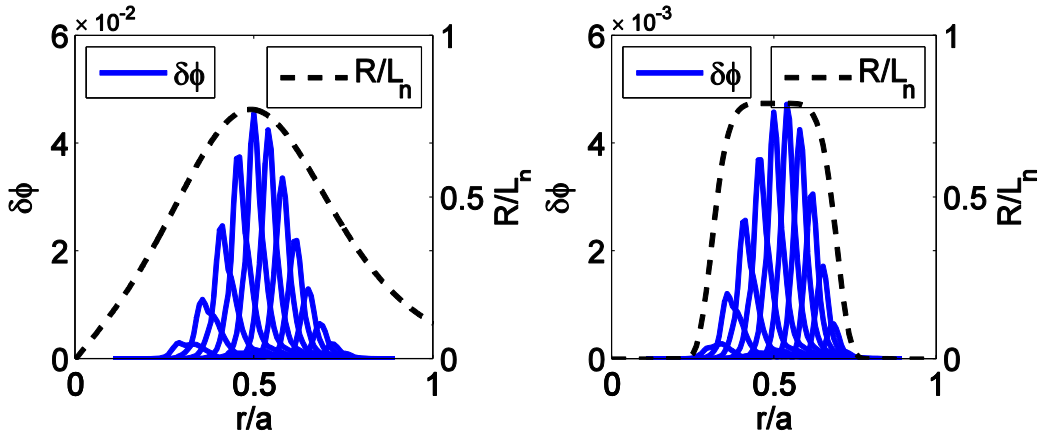

(a) (b)

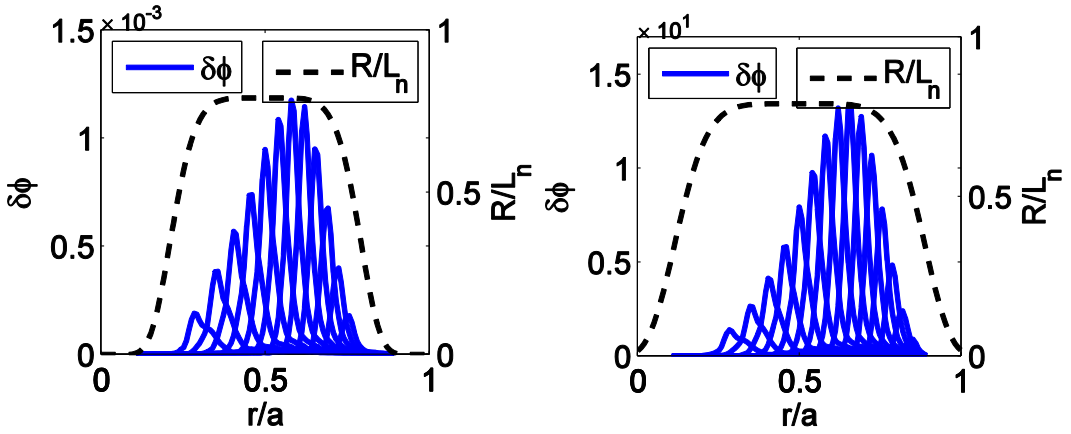

(c) (d)

Figure 2: Radial mode structure of KBM (blue solid curves) for different density/temperature gradient profiles: (a) global profile, (b) $r_w = 0.2$a, (c) $r_w = 0.3$a, (d) $r_w = 0.4$a

III. Linear Theory of the KBM

Here we introduce a linear theory for explaining the sensitivity of the KBM instability and its mode structure to the width of the local plasma radial gradient. Using the ballooning representation and s − α equilibrium model, we can write the normalized eigenmode equation for the KBM [4, 6]:

$$\frac{\partial}{\partial\theta}\left[1+\left(s\theta-\alpha\sin\theta\right)^2\right]\frac{\partial\delta\Psi}{\partial\theta}+\frac{\alpha}{4\grave{o}_n\left(1+\eta\right)}\left[\left(\Omega-1\right)\left(\Omega-f\left(\theta\right)\right)\right.$$
$$\left.+\eta_e f\left(\theta\right)-\frac{\left(\Omega-1\right)^2}{1+\tau-\tau I}+\tau\frac{\partial}{\partial\theta}H\frac{\partial}{\partial\theta}\right]\delta\Psi=0 \qquad (1)$$

Where only the lowest order of the parallel ion current is retained, and θ is the ballooning angle with respect to the field line, q is the safety factor, $\tau = T_e/T_i$ is the electron/ion temperature ratio, $\epsilon_n = \frac{L_n}{R}$ is the inverse of the normalized density gradient, $\eta_e = \frac{dlnT_e}{dlnn_e}$ and $\Omega = \frac{\omega}{\omega_{*e}}$ is the mode frequency normalized by the electron diamagnetic frequency $\omega_{*e} = \frac{k_\theta cT_e}{eBL_n}$, and $\delta\Psi$ is the perturbed field which is an even function of θ. The functions $f(\theta)$, I and H are defined by

$$f(\theta) = 2\grave{o}_n \left[\cos\theta + (s\theta - \alpha\sin\theta)\sin\theta\right], \tag{2}$$

$$I = \frac{\omega - \omega_{*i}}{\omega - \omega_{di}} F_i J_0^2 (\Lambda_i)_{\nu} \ , \tag{3}$$

$$H = \frac{1}{\omega_{*e}^2 q^2 R^2} \left\langle \frac{\omega - \omega_{*i}}{\omega - \omega_{di}} v_{\square}^2 F_i J_0^2 (\Lambda_i) \right\rangle_{\nu} , \tag{4}$$

where Λ_i , $\widehat{\omega_{*\iota}}$, and $\widehat{\omega_{d\iota}}$ can be expressed as

$$\Lambda_{\mathrm{i}} = \sqrt{2} k_\theta \rho_i \sqrt{1 + (s\theta - \alpha\sin\theta)^2}\, v_\perp / v_T \,, \tag{5}$$

$$\omega_{*_i} = -\frac{\omega_{*_e}}{\tau}\left[1 + \eta_i \left(\frac{m_i v_{\square}^2 + m_i v_\perp^2}{2T_i} - \frac{3}{2}\right)\right], \tag{6}$$

$$\omega_{di} = -\frac{\omega_{*_e}}{\tau} f(\theta)\left(\frac{m_i v_{\square}^2}{2T_i} + \frac{m_i v_\perp^2}{4T_i}\right). \tag{7}$$

Here F_i is the Maxwellian distribution function for the ions, $v_T = \sqrt{\frac{2T_i}{m_i}}$ is the ion thermal velocity, $\rho_i = \frac{v_T}{\omega_{ci}} = \frac{v_T m_i c}{eB}$ is the ion Larmor radius of ion, J_0 is the zeroth order Bessel function, and $\langle \cdots \rangle_v$ denotes the velocity space integral. For simplicity, we assume τ=Te/Ti=1, and $\eta = \eta_e = \eta_i$. Note that the perturbed parallel ion current, essentially given by the term H in Eq. (1), is inversely proportional to q^2.

To solve Eq. (1), a numerical nonlinear eigenvalue code is developed to find the eigenvalue, i.e., the normalized frequency Ω. The perturbed field $\delta\Psi$ is then represented by a discrete vector, and thus Eq. (1) could be transformed to a matrix form. The resulting discrete nonlinear eigenmode equation can be solved iteratively. The integral I(θ) and H(θ) are related to the standard plasma dispersion relation function

$$\mathrm{Z}(\zeta) = \int \frac{\exp(-\mathrm{z}^2)}{\mathrm{z} - \zeta} \mathrm{dz} \,, \tag{8}$$

which can be expressed in terms of the complex error function, which can be

evaluated accurately and rapidly using the basis function method and the Fast Fourier Transformation (FFT) [19, 20].

IV. Effect of the Perturbed Parallel Ion Current

In order to show the effect of the perturbed parallel ion current, we use the preceding theory to compare the KBM results for with or without the perturbed parallel ion. Fig. 3 shows the resulting growth rates and real frequencies normalized by the electron diamagnetic frequency ω_{*e} for: $s = 0.4$, $b_0 = (k_\theta \rho_i)^2 = 0.01$, $\eta = 2$, $q = 2$, $\epsilon_n = 0.175$. Fig. 3 also shows that the parallel ion current provides a stabilizing effect that reduces the growth rate of the KBM in the IBM (ideal MHD ballooning mode) unstable regime.

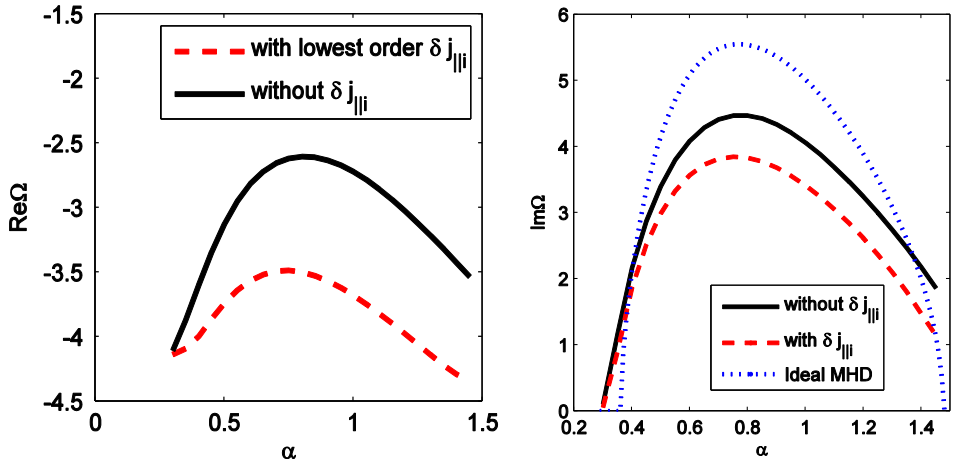

(a) (b)

Figure 3: The growth rate and real frequency vs. α for cases with or without the perturbed parallel ion current term (red dashed and the black solid curves, respectively), and of the ideal MHD ballooning mode (blue dotted curve).

Fig. 4 shows the eigenfunctions along the parallel direction for the cases with or without the perturbed parallel ion current, where only half the eigenfunction is shown since the mode structures are even in θ. The value of the perturbed field at $\theta = 0$ is set to unity for simplicity and the simulation parameters are the same as in Fig. 3. In the MHD unstable region, the eigenfunction is confined around the outside middle plane with θ=0. We also note that the most unstable region is around that with the bad curvature, or $\theta = 0, 2\pi, 4\pi, ...$, and the least unstable region is around that with the

good curvature, or $\theta = \pi, 3\pi, ...$, which is consistent with the ballooning assumption of the theory. The parallel perturbed ion current can broaden the mode structure, i.e., more perturbed field energy moves away from the most unstable ballooning angles, which means the perturbed energy moves away from the bad curvature region, thereby leading to stabilization by the perturbed parallel ion current.

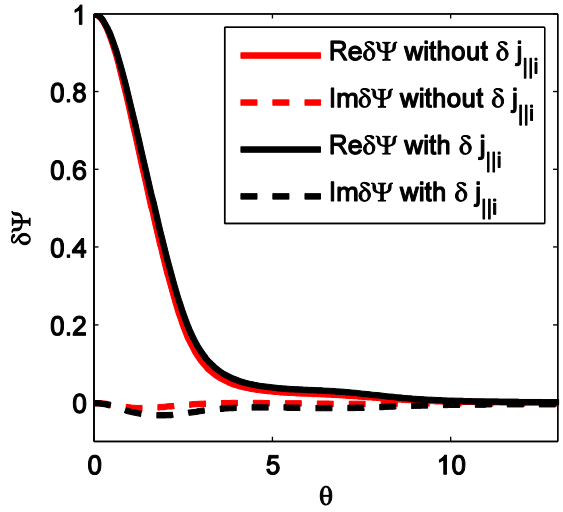

Figure 4: Comparison of eigenmode structure with or without perturbed parallel ion current in ballooning space, with α=0.8.

As mentioned, the perturbed parallel ion current is inversely proportional to the square of the safety factor and it can stabilize the KBM. The safety factor profile used here has normal shear. At larger radial position the safety factor q is larger, and the stabilization effect of the perturbed parallel ion current becomes weaker. Thus the growth rate of the linear eigenmode increases in the radially outward direction, which induces the outward shift of the radial mode structure in Fig.2.

V. Magnetic Shear Effect on the KBM

It has also been found that the KBM will be unstable due to the interchange drive when magnetic shear is small and pressure gradient is sufficiently small []. In the preceding section, we have studied the normal shear. In this section, we examine the KBM mode structure with reversed magnetic shear. The q profile in our GTC simulation is a parabolic function of r [21], or $q(r) = q_{mid} + c\left(\frac{r}{a} - 0.5\right)^2$. So the magnetic shear increases monotonically with r and poloidal flux ψ_p near $r = a/2$,

where s=0 and $q = q_{mid}$ at $r = a/2$. The density and temperature gradient profile still have the flat profile with $r_w = 0.3$. The GTC simulation result is shown in Fig. 5, for $\beta = 2.0\%$, $\alpha = 0.73$, $k_\theta \rho_s = 0.2$, $n = 10$ and $q = 1.4$, $s = 0.81$, $\frac{R}{L_n} = 2.2$, $\frac{R}{L_T} = 7.0$ at $r = \frac{a}{2}$, with the q profile given by $q_{mid} = 1.4$ and $c = 4.0$. Consistent with previous studies[6], the linear mode from the GTC simulation is mostly unstable around r=0.5a, where the magnetic shear s is very small and the growth rate is much larger than that in other radial positions, as can be seen in Fig. 5.

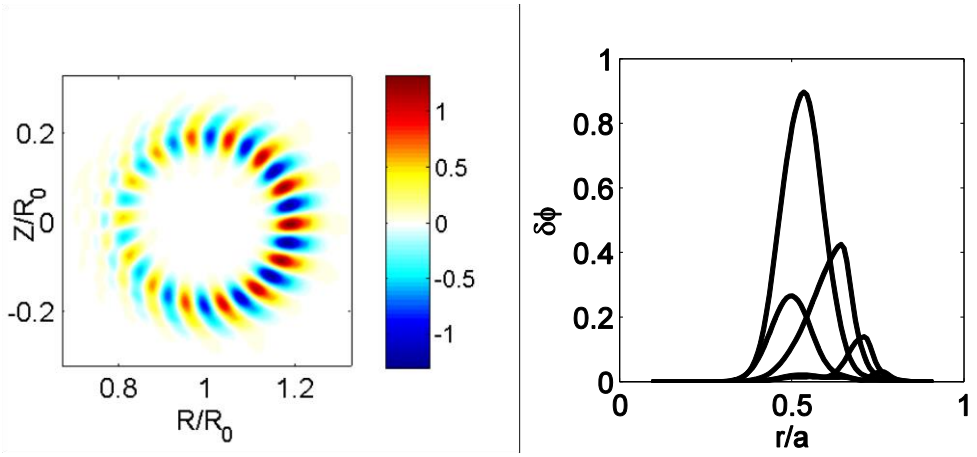

(b) (b)

Figure 5: (a) Mode structure with n=10 in poloidal plane and (b) radial mode structure obtained by the GTC simulation for a reversed shear configuration.

Our eigenvalue solver can also be used to investigate the magnetic shear effect on the KBM for cases with and without the perturbed parallel ion current. Fig.6 shows results for $\alpha = 0.3$, $\mathrm{k}_\theta \rho_s = 0.1$, $\eta_i = \eta_e = 0.175$, $L_n/R = 0.175$, $q = 2$. It is found that the linear frequency and growth rate are strongly affected by the magnetic shear. When the perturbed parallel ion current is ignored, the growth rate increases rapidly with s when s<0, and decreases relatively slowly for s>0. This result is consistent with that from our GTC simulation in Fig. 5, where the radial mode structure is restrained around zero-shear point. The growth rate of the unstable poloidal mode increases sharply for s<0, and decreases slowly for s>0.

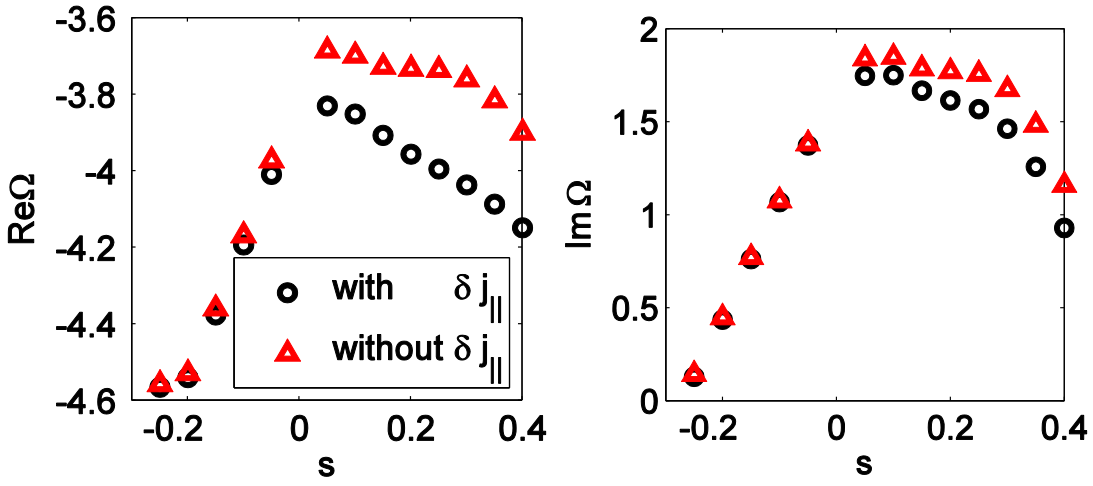

(a) (b)

Figure 6: Dependence of the frequency and growth rate on the magnetic shear s for with or without perturbed parallel ion current

VI. Effect of Perturbed Parallel Ion Current for Different Magnetic Shears

In this section, we discuss the effect of perturbed parallel ion current for different magnetic shears. Fig. 6 also shows that in the positive shear region the perturbed parallel ion current can provide stability for the KBM, but it doesnot affect the linear frequency and growth rate in the negative shear region. To verify this phenomenon, we consider two different q profiles for our GTC simulation, that have constant positive and negative shears in the central region of the simulation domain. Setting $q\left(\frac{a}{2}\right)=1.4$ and using the relationship $s=\frac{r}{q}\frac{dq}{dr}$, we can obtain the q profile from the magnetic shear profile $s(r)$：：

$$s(r)=\begin{cases} -\frac{s_{mid}}{r_l^2}\left(r-r_l\right)^2+s_{mid} & 0<r<r_l \\ s_{mid} & r_l<r<r_r \\ \frac{s_{max}-s_{mid}}{\left(a-r_r\right)^2}\left(r-r_r\right)^2+s_{mid} & r_r<r<a \end{cases}, \qquad (9)$$

where s_{mid} is the constant magnetic shear in the central region for simulating the local limit, $r_l<r<r_r$, $r_l+r_r=$ a, $r_r-r_l=r_w$ indicateing the width of local profile, and s_{max} is the magnetic shear at $r=a$ position. The density and temperature gradient profiles are still the local profile used earlier. To show the perturbed parallel ion current effects with positive and negative shears, the GTC

simulation is carried out for $s_{mid} = 0.81$ and $s_{mid} = -0.2$, respectively, with the other parameters the same as that in Sec. V.

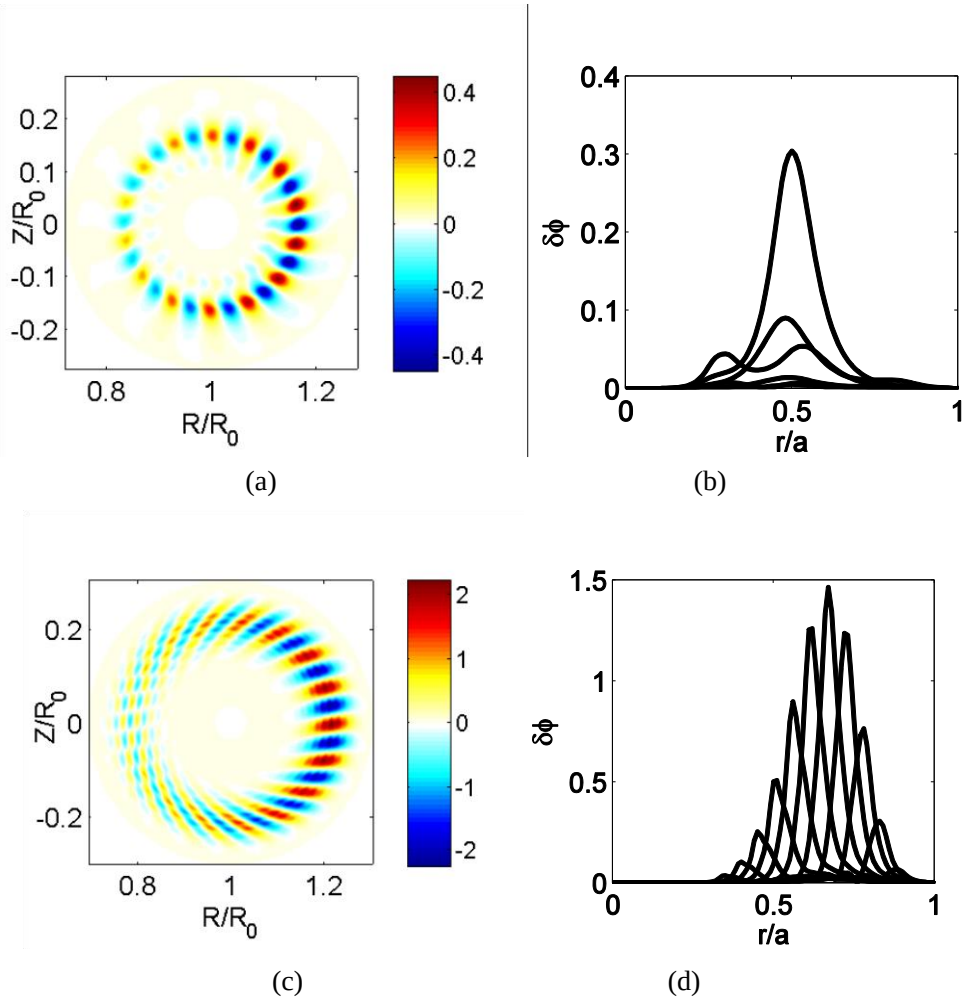

Figure 7: Mode structure in poloidal plane and radial mode structure with (a) (b) $s_{mid} = -0.2$, (c) (d) $s_{mid} = 0.81$.

As shown in the Fig. 7(c-d), the radial mode structure centered at $r = a/2$ for the negative shear case, but it moves outward for the positive shear case. The different behaviors of the KBM mode structure for different magnetic shears are fully consistent with that predicted by the theory given in the last section, namely, the perturbed parallel ion current provides stability for the KBM mode for s>0, and it doesn't affect the KBM stability when s<0.

VII. CONCLUSION AND DISCUSSION

In this work, we have investigated the KBM instability using the gyrokinetic simulation with the GTC code. We found that the linear growth rate and frequency are

affected by the locality of the plasma profile, or the size of the simulation window. The poloidal mode structure moves outward in the radial direction for the normal magnetic shear while it doesnot move for the negative magnetic shear. A linear eigen mode theory is proposed to explain this radial shift of the KBM. It is found that the perturbed parallel ion current, ignored in the existing theories, [4] affects the growth rate differently for positive and negative shears. For positive magnetic shear, it provides stability to the KBM and decreases its growth rate. However, for negative magnetic shear, the perturbed parallel current does not affect the growth rate at all. These theoretical results fully explain that of the GTC simulation.

ACKNOWLEDGEMENT

The work is supported by National Magnetic Confinement Fusion Energy Research Program under Grant No. 2015GB110000, 2013GB111000, China NSFC under Grant No. 11575158, the Recruitment Program of Global Youth Experts. Y. Y. Li would like thank H. S. Xie, H. T. Chen W. Chen for the useful discussions. Y. Xiao is grateful for the helpful discussions with Professors Z. Lin, L. Chen and M.Y. Yu.

REFERENCES

[1] C. H. Ma, X. Q. Xu. Global kinetic ballooning mode simulations in BOUT++[J]. Nuclear Fusion, 2016, 57(1): 016002.

[2] W. M. Tang , J. W. Connor, R. J. Hastie. Kinetic-ballooning-mode theory in general geometry[J]. Nuclear Fusion, 1980, 20(11): 1439.

[3] F. Zonca, L. Chen, R. A. Santoro. Kinetic theory of low-frequency Alfvén modes in tokamaks[J]. Plasma physics and controlled fusion, 1996, 38(11): 2011.

[4] A. Hirose, L. Zhang, M. Elia. Higher order collisionless ballooning mode in tokamaks[J]. Physical review letters, 1994, 72(25): 3993.

[5] A. Hirose, M. Elia. Kinetic ballooning mode with negative shear[J]. Physical review letters, 1996, 76(4): 628.

[6] A. Hirose, M. Elia. Kinetic ballooning stability of internal transport barriers in tokamaks[J]. Physics of Plasmas, 2003, 10(10):1195-1198.

[7] I. Holod, D. Fulton, Z. Lin. Microturbulence in DIII-D tokamak pedestal. II. Electromagnetic instabilities[J]. Nuclear Fusion, 2015, 55(9): 093020.
[8] Y. Chen, S. E. Parker, W. Wan, R. Bravenec. Benchmarking gyrokinetic simulations in a toroidal flux-tube[J]. Physics of Plasmas (1994-present), 2013, 20(9): 092511.
[9] A. Bottino, B. Scott, S. Brunner, B. F. McMillan, T. M. Tran, T. Vernay, L. Villard, S. Jolliet, R. Hatzky, and A. G. Peeters. Global nonlinear electromagnetic simulations of tokamak turbulence[J]. IEEE Transactions on Plasma Science, 2010, 38(9): 2129-2135.
[10] A. Mishchenko, R. Hatzky, A. Könies. Global particle-in-cell simulations of Alfvénic modes[J]. Physics of Plasmas (1994-present), 2008, 15(11): 112106.
[11] E. A. Belli, J. Candy. Fully electromagnetic gyrokinetic eigenmode analysis of high-beta shaped plasmas[J]. Physics of Plasmas (1994-present), 2010, 17(11): 112314.
[12] T. Görler, N. Tronko, W. A. Hornsby, A. Bottino, R. Kleiber, C. Norscini, V. Grandgirard, F. Jenko, and E. Sonnendrücker. Intercode comparison of gyrokinetic global electromagnetic modes[J]. Physics of Plasmas (1994-present), 2016, 23(7): 072503.
[13] H. S. Xie, Y. Xiao, I. Holod, Z. Lin, E. A. Belli. Sensitivity of kinetic ballooning mode instability to tokamak equilibrium implementations[J]. Journal of Plasma Physics, 2016, 82(5).
[14] W. W. Lee. Gyrokinetic approach in particle simulation[J]. Physics of Fluids (1958-1988), 1983, 26(2): 556-562.
[15] Z. Lin, T. S. Hahm, W. W. Lee, W. M. Tang, R. B. White. Turbulent transport reduction by zonal flows: Massively parallel simulations[J]. Science, 1998, 281(5384): 1835-1837.
[16] Z. Lin, L. Chen. A fluid–kinetic hybrid electron model for electromagnetic simulations[J]. Physics of Plasmas (1994-present), 2001, 8(5): 1447-1450.
[17] Y. Xiao, I. Holod, Z. Wang, Z. Lin, T. Zhang. Gyrokinetic particle simulation of microturbulence for general magnetic geometry and experimental profiles[J]. Physics of Plasmas (1994-present), 2015, 22(2): 022516.
[18] I. Holod, W. L. Zhang, Y. Xiao, Z. Lin. Electromagnetic formulation of global gyrokinetic particle simulation in toroidal geometry[J]. Physics of Plasmas (1994-present), 2009, 16(12): 122307.
[19] J. A. C. Weideman. Computation of the complex error function[J]. SIAM Journal on Numerical Analysis, 1994, 31(5): 1497-1518.
[20] Ö. D. Gürcan. Numerical computation of the modified plasma dispersion function with curvature[J]. Journal of Computational Physics, 2014, 269: 156-167.
[21] W. Deng, Z. Lin. Properties of microturbulence in toroidal plasmas with reversed magnetic shear[J]. Physics of Plasmas (1994-present), 2009, 16(10): 102503.